

An *agr*-Like Two-Component Regulatory System in *Lactobacillus plantarum* Is Involved in Production of a Novel Cyclic Peptide and Regulation of Adherence

Mark H. J. Sturme,^{1,2*} Jiro Nakayama,⁴ Douwe Molenaar,^{1,3} Yoshiko Murakami,⁴
Ryoko Kunugi,⁴ Toshio Fujii,² Elaine E. Vaughan,^{1,2} Michiel Kleerebezem,^{1,3}
and Willem M. de Vos^{1,2}

Wageningen Centre for Food Sciences, Wageningen, The Netherlands¹; Laboratory of Microbiology,
Wageningen University, Wageningen, The Netherlands²; NIZO Food Research, Ede,
The Netherlands³; and Department of Bioscience and Biotechnology,
Faculty of Agriculture, Kyushu University, Fukuoka, Japan⁴

Received 20 January 2005/Accepted 4 May 2005

We have analyzed a locus on the annotated *Lactobacillus plantarum* WCFS1 genome that showed homology to the staphylococcal *agr* quorum-sensing system and designated it *lam* for *Lactobacillus agr*-like module. Production of the *lamBDCA* transcript was shown to be growth phase dependent. Analysis of a response regulator-defective mutant ($\Delta lamA$) in an adherence assay showed that *lam* regulates adherence of *L. plantarum* to a glass surface. Global transcription analysis of the wild-type and $\Delta lamA$ strains in early, mid-, and late log phase of growth was performed using a clone-based microarray. Remarkably, only a small set of genes showed significant differences in transcription profiles between the wild-type and *lamA* mutant strains. The microarray analysis confirmed that *lamBDCA* is autoregulatory and showed that *lamA* is involved in regulation of expression of genes encoding surface polysaccharides, cell membrane proteins, and sugar utilization proteins. The *lamBD* genes encoding the putative autoinducing peptide precursor (LamD) and its processing protein (LamB) were overexpressed using the nisin-controlled expression system, and culture supernatants were analyzed by liquid chromatography/mass spectrometry (LC/MS) to identify overproduced LamD-derived peptides. In this way, a cyclic thiolactone pentapeptide that possesses a ring structure similar to those of autoinducing peptides of the staphylococcal *agr* system was identified. The peptide was designated LamD558, and its sequence (CVGIW) matched the annotated precursor peptide sequence. Time course analysis of wild-type culture supernatants by LC/MS indicated that LamD558 production was increased markedly from mid-log to late log growth phase. This is the first example of an *agr*-like system in nonpathogenic bacteria that encodes a cyclic thiolactone autoinducing peptide and is involved in regulation of adherence.

Regulation of physiological changes in bacterial populations in many cases has been shown to be dependent on specific cell densities and growth phases. This phenomenon of cell density-dependent gene expression has been termed quorum sensing and was initially found to regulate bioluminescence in *Vibrio fischeri* (15). Since then, a large variety of quorum-sensing systems has been discovered in both gram-negative and gram-positive bacteria (29). Well-studied examples of quorum sensing-regulated features in gram-positive bacteria include genetic competence in *Bacillus subtilis* (55) and *Streptococcus pneumoniae* (8), virulence and biofilm formation in *Staphylococcus aureus* (39, 65) and *Enterococcus faecalis* (16, 44), and the production of antimicrobial peptides, including bacteriocins and lantibiotics, in various lactic acid bacteria (26, 38). To regulate these quorum-sensing systems, bacteria produce extracellular signaling molecules that are responsible for cell-to-cell communication. While many gram-negative bacteria communicate via *N*-acyl-homoserine lactones, peptides are the most common and well-studied signaling molecules in gram-

positive bacteria; here these peptides are referred to as autoinducing peptides (AIPs). These peptides have diverse structures but share a small size, ribosomal synthesis, and—in many cases—are subject to specific posttranslational modifications that add to their stability, specificity, and functionality. The exported AIPs regulate quorum sensing via two-component regulatory systems (TCS), consisting of histidine protein kinase and response regulator genes (26, 54).

Lactobacilli are commonly used in fermentations of dairy, meat, and vegetable foods (7, 47), but several species are also common inhabitants of the human gastrointestinal tract (58). One of these is *Lactobacillus plantarum* (1), which is a versatile species that is encountered in diverse environmental niches, such as fermented food products, plant material, and the human gastrointestinal tract (1, 13, 14). *L. plantarum* WCFS1 is a single colony isolate of the esophageal *L. plantarum* strain NCIMB8826 (17), which was shown to survive stomach passage in an active form and to persist for up to 7 days in the human gastrointestinal tract after a single dose (6, 59). The *L. plantarum* WCFS1 genome sequence has been completed and appears to be one of the largest genomes known among lactic acid bacteria (27). The 3.3-Mb genome encodes a large repertoire of extracellular proteins, sugar and amino acid import and utilization proteins, and many regulatory genes, including

* Corresponding author. Mailing address: Laboratory of Microbiology, Wageningen University, Hesselink van Suchtelenweg 4, 6703 CT Wageningen, The Netherlands. Phone: 31-317-483113. Fax: 31-317-483829. E-mail: mark.sturme@wur.nl.

TABLE 1. Bacterial strains and plasmids used in this study

Bacterial strain or plasmid	Relevant property ^a	Reference(s) or source
<i>E. coli</i> JM109	Cloning host for pUC19ery and its derivatives	Promega 17
<i>L. plantarum</i> WCFS1	Wild type; single colony isolate from human saliva isolate NCIMB8826	This work
<i>L. plantarum</i> WCFS1::pLAMA-K28	<i>L. plantarum</i> WCFS1 with single chromosomal integration of pLAMA-K28	This work
<i>L. plantarum</i> MSΔlamA	DCO mutant in <i>L. plantarum</i> WCFS1 with <i>lamA</i> replaced by <i>lamA</i> ::tag gene replacement cassette	This work
<i>L. plantarum</i> NCIMB8826 Int-1	Em ^r , stable <i>nisRK</i> integrant in the tRNA ^{Ser} locus, after transformation with pMEC10	41
<i>L. plantarum</i> MS18048	Em ^r Cm ^r ; <i>L. plantarum</i> NCIMB8826 Int-1 containing pNZ8048	This work
<i>L. plantarum</i> MSI011	Em ^r Cm ^r ; <i>L. plantarum</i> NCIMB8826 Int-1 containing pNICE011	This work
pUC19ery	Amp ^r Em ^r ; 3.8-kb derivative of pUC19 containing 1.1-kb HinPI fragment of pIL253 carrying the Ery ^r gene	57
pLAMA-K28	pUC19ery vector carrying <i>lamA</i> ::tag gene replacement cassette	This work
pNZ8048	A derivative of the pNZ8030 series containing P _{<i>nisA</i>} , a MCS, and T _{<i>pepN</i>} . NICE vector, Cm ^r	9, 41
pNICE011	<i>lamBD</i> translationally fused (NcoI) to pNZ8048, Cm ^r	This work
pBACe3.6	Bacterial artificial chromosome plasmid	

^a Em^r, erythromycin resistant; Cm^r, chloramphenicol resistant; Amp^r, ampicillin resistant; DCO, double crossover; MCS, multiple cloning site.

13 TCS. These may aid the persistence and survival of this highly adaptive microbe in diverse ecological niches (27).

Here we describe the functional analysis of an annotated two-component regulatory system of *L. plantarum* WCFS1 (27) that shows homology to the *agrBDCA* and *fsrABC* quorum-sensing systems of *Staphylococcus aureus* (21) and *Enterococcus faecalis* (34), respectively (Fig. 1). The latter quorum-sensing systems are involved in regulation of virulence factor production, mainly via the production of extracellular proteins (40, 44). In addition, they are also involved in biofilm formation (16, 60, 65). The *agr* system in staphylococci encodes the two-component histidine protein kinase AgrC and response regulator AgrA, an AIP derived from precursor peptide AgrD, and additionally AgrB, a protein that is involved in processing and posttranslational modification of AgrD (66, 67). The corresponding regulatory proteins and a fused FsrBD protein can also be found in the *fsr* system (34, 45). The AIPs produced from the precursor peptide AgrD are cyclic thiolactone peptides in staphylococci (21), while in *E. faecalis* the C-terminal part of FsrBD encompasses the cyclic lactone gelatinase biosynthesis-activating pheromone (GBAP) (34). One of the *L. plantarum* TCS showed a genetic organization similar to that of the *agr* system and was designated *lam* for *Lactobacillus agr*-like module. The function and expression of the *lam* system were studied by a global genomics approach, and *lam* was found to be involved in regulation of adherence to a glass surface. Moreover, the production of a novel *agr*-like cyclic thiolactone pentapeptide could be established by homologous overexpression of the *lamBD* genes.

MATERIALS AND METHODS

Bacterial strains and growth media. The bacterial strains and plasmids used in this study and their characteristics are shown in Table 1. *Escherichia coli* JM109 was cultivated at 37°C aerobically in Luria-Bertani broth or in brain heart infusion broth when selecting for erythromycin resistance (Difco). *Lactobacillus plantarum* WCFS1 and its derivatives were cultivated in Man-Rogosa-Sharpe broth (MRS; Difco) at 30°C without agitation (unless stated differently). Solid media contained 1.5% (wt/vol) agar. Where appropriate, antibiotics were added as follows: erythromycin, 150 μg ml⁻¹ (*E. coli*) or 5 μg ml⁻¹ (*L. plantarum* WCFS1); chloramphenicol, 25 μg ml⁻¹ (*E. coli*) or 10 μg ml⁻¹ (*L. plantarum* WCFS1).

DNA isolation and construction of integration plasmids. Genomic DNA was isolated from 10-ml logarithmic-phase cultures of *L. plantarum* WCFS1 essentially as described previously (4), with additional disruption by bead beating in a Biospec bead-beater (three times for 90 s each time at 5,000 rpm) and purification by phenol-chloroform extractions and isopropanol precipitation. PCR was performed using proofreading Platinum Pfx DNA polymerase (Invitrogen) and using genomic DNA or plasmid pBACe3.6 (generously provided by J. Catanese) as a template. Primers WCFS-lamA-NdeI and WCFS-lamA-EcoRI and primers WCFS-lamA-KpnI and WCFS-lamA-BamHI were used to amplify the 5' and 3' ends of *lamA* and the regions flanking *lamA* (approximately 1 kb on each side), whereas primers pBAC-SacB-EcoRI and pBAC-SacB-KpnI was used to amplify a locus-tagging sequence that was cloned between these two fragments (Table 2). PCR products were cloned into the nonreplicating integration vector pUC19ery, after digesting the PCR products and vector with the appropriate restriction enzymes (Gibco BRL) (57). Plasmids were transformed into *E. coli* JM109 by a heat shock procedure as recommended by the manufacturer (Promega). This resulted in plasmid pLAMA-K28 containing the complete gene replacement cassette with the mutated response regulator gene.

Gene replacement of the *L. plantarum* WCFS1 *lamA* gene. *L. plantarum* WCFS1 was transformed by electroporation, essentially as previously described (22), using electrocompetent cells of *L. plantarum* that were grown in MRS supplemented with 1% glycine and prepared in 30% polyethylene glycol-1450. *L. plantarum* cells were transformed with 2 μg of integration plasmid pLAMA-K28, and integrants were selected by plating on MRS agar supplemented with erythromycin and incubation in an anaerobic jar at 30°C for 2 to 4 days. Single colonies were analyzed by colony PCR with plasmid chromosome crossover junction primers Lam-NdeI-junction-1 and SacB-control-2 or SacB-control-3 and Lam-BamHI-junction-4 (Table 2) to confirm single crossover integration up- or downstream of the mutation locus. For this purpose, single colonies were suspended in 20 μl Tris-EDTA and cells were disrupted by a microwave treatment for 3 min at 750 W and subsequent incubation for 10 min at 95°C, after which PCR analysis was performed. A single crossover mutant was selected and designated *L. plantarum* WCFS1::pLAMA-K28. This mutant was subsequently propagated for 200 generations in MRS without erythromycin to obtain the anticipated erythromycin-sensitive (Em^s) *lamA*::tag replacement mutant after a second homologous recombination event. The anticipated gene organization of the *lamA*::tag locus in the obtained gene replacement mutant (MSΔlamA) was verified by colony PCR with crossover junction primers and *lamA*-flanking primers RR-lamA-F and RR-lamA-R as described above (primers shown in Table 2), as well as by Southern blot analysis using standard procedures (50).

RNA extraction. Cultures of the wild-type and *lamA* mutant strains were aerobically grown in 100 ml MRS at 30°C starting from an optical density at 600 nm (OD₆₀₀) of 0.3. Samples (25 ml) were harvested at early, mid-, and late logarithmic growth phases, immediately quenched, and mixed in 4 volumes of quenching buffer at -80°C to stop further transcription (60% methanol, 66.7 mM HEPES, pH 6.5), as described recently (42). Subsequently, samples were pelleted by centrifugation at -20°C in a prechilled centrifuge and cells were resuspended in 0.5 ml cold Tris-EDTA buffer. RNA was isolated by the Macaloid

TABLE 2. Primers used in this study

Primer	Sequence (5'-3') ^a
WCFS-lamA-NdeIcagtgatt catatg TTGACCGGATGTTATCCAG
WCFS-lamA-EcoRIcat gaattc ATTGGACAAGCACTTGCGACG
WCFS-lamA-KpnIacgggt acc TTAGTAATGATTTGCCG
WCFS-lamA-BamHIaa tgatcc AGATCATTTGGCGAGTTTAG
pBAC-SacB-EcoRIcg taattc TACTGACTATTCCG
pBAC-SacB-KpnItc aggtacc GTGTTTGAAGTGATCAGC
Lam-NdeI-junction-1GTTAGCCAAGTTACTTTGC
Lam-BamHI-junction-4CTACGCTTATTGGTACGAGC
SacB-control-2CATCGATAAACTGCTGAACG
SacB-control-3CGATGCTGAGTTAGCGAACG
RR-lamA-FGCAGGCGACTTCCTTGAAC
RR-lamA-RGAAGCGAGTATCTCAGAATG
LamBD-NICE-KpnICTAGGT acc TTATTTACGTAGTTTCGTC
LamBD-NICE-NcoIGGAGTGGG ccat GGAAAAGCCAGAAC
pNZ8048-FGTTAGATACAATGATTTTCGTTTCG (left of MCS)
pNZ8048-RCAATTGAACGTTTCAAGCCTTGG (right of MCS)
Lp1197-2F ^bGACAAGCACGACCAACTCACA
Lp1197-2R ^bTAAGCCGACAACCTAGCCCAATCAA
Lp1204-1F ^bACGTCATCCATTTTCGTTTTT
Lp1204-1R ^bGTCTCATTCACGCATCTCTGT
Lp3581-2F ^bGATTGGCCTATTGTGATT
Lp3581-2R ^bGAGCTTCGATTTCATTCA

^a Nucleotides homologous to nucleotides in the genome sequence are shown in capital letters, nucleotides in the restriction enzyme recognition sequence are shown in bold type, and nonhomologous nucleotides are shown in lowercase letters. Mismatched nucleotides are in italics; the start codon of LamBD is underlined. MCS, multiple cloning site.

^b Primers used for real-time PCR.

method, essentially as described previously (28), and further purified by on-column DNase I treatment on RNeasy columns (QIAGEN). For DNA microarray analysis, 25- μ g RNA aliquots were prepared. All experiments were performed in duplicate.

Northern blot analysis of *lamBDCA* gene expression. RNA was isolated as described above and 10.0- μ g RNA sample or 3.0- μ l RNA size marker (Invitrogen) was used for Northern blot analysis by glyoxal denaturation as described previously (50). RNA was fixed to the membrane by auto-cross-linking in an UV Stratilinker, and Northern hybridization was performed overnight at 65°C in QuikHyb hybridization buffer (Stratagene) as described previously (50). Blots were analyzed by exposure to Phosphor screens (Molecular Dynamics) and scanned on a Storm Image scanner (Molecular Dynamics). DNA probes were made using a nick translation kit (Invitrogen). Signal intensities were quantified for a *lamC* internal probe and normalized against the 16S rRNA signal intensities.

Adherence assays. Adherence phenotype characterization and cell aggregation were initially performed with strains grown in polystyrene petri dishes (6-cm diameter) containing glass cover slides and 5 ml MRS by the method of Merritt et al. (33). For quantitative measurements, strains were grown in 1 ml MRS in 24-well plates (Techno Plastic Products, Switzerland), with glass cover slides (14-mm diameter; Menzel-Glazer) on the bottom of the wells. Wells containing medium only were used as blanks, and a separate plate was used for optical density measurements. Cells were grown for 24 or 48 h at 30°C after which medium was removed. Wells were washed twice with phosphate-buffered saline to remove loosely attached cells, and the remaining adhered cells were air dried for 10 min. For staining, 0.5 ml crystal violet (0.1% in deionized water) was added and incubated for 30 min at 22°C. Wells were washed three times with deionized water, and the stained attached cells were removed by dissolving them in 1 ml 96% ethanol. Absorbance was measured at 595 nm, with six replicates for each strain. Experiments were performed independently three times, and the statistical significance of differences was calculated using the Student's *t* test (two-tailed, two-sample equal variance).

Array design. For transcription profiling, clone-based DNA microarrays were used; these microarrays were based on clones derived from the genomic library that was previously constructed for genome sequencing of *L. plantarum* WCFS1 (27). In total, 3,692 genomic fragments were PCR amplified from the genomic library using Superaq (SphaeroQ, Leiden, The Netherlands) and vector-derived universal forward and reverse primers with 5'-C6 aminolinkers to facilitate cross-

linking to the aldehyde-coated glass slides. The resulting amplicons had an average size of 1.2 kb, covered 80.8% of the genome, and represented 2,683 of the 3,052 annotated genes (88%). They were purified by ethanol precipitation and dissolved in 3 \times SSC (1 \times SSC is 0.15 M NaCl plus 0.015 M sodium citrate). Subsequently, the purified amplicons were arrayed in a controlled atmosphere on CSS-100 silylated aldehyde glass slides with quill pins (Telechem, SMP3) in an SDDC 2 Eurogridder (ESI, Toronto, Canada). Afterwards the slides were dried and blocked with borohydride.

cDNA preparation, fluorescent labeling, and hybridization. Differential transcript levels were determined by two-color (Cy5 and Cy3) fluorescence hybridizations of the corresponding cDNAs on the clone-based DNA microarray. Cy5/Cy3 dye swaps were performed for the wild-type and *lamA* mutant cDNA samples. Labeled cDNAs were prepared according to protocols from Stanford University (Patrick O. Brown's laboratory [http://cmgm.stanford.edu/pbrown/protocols/index.html]) using random hexamers for reverse transcription. Total RNA (25 μ g) was labeled during reverse transcription by incorporation of FluoroLink Cy3- or Cy5-labeled dUTP (Amersham Biosciences) using a reverse transcription kit (Gibco BRL). The reaction was stopped by adding 1 N NaOH and neutralized with 1 M HCl. Unincorporated dye was removed from labeled fragments by using Autoseq G50 columns (Amersham Biosciences). Slides were prehybridized for 45 min at 42°C in 20 ml filtered prehybridization solution (1% bovine serum albumin, 5 \times SSC, and 0.1% sodium dodecyl sulfate), washed in filtered deionized water, and dried. Cohybridization of Cy5- and Cy3-labeled cDNA probes was performed overnight at 42°C in Easyhyb buffer (Roche) according to the manufacturer's protocol. The slides were washed twice in 1 \times SSC and 0.2% sodium dodecyl sulfate, once in 0.5 \times SSC, and twice in 0.2 \times SSC at 37°C. The slides were dried before scanning.

Microarray scanning and data analysis. Slides were scanned on a ScanArray Express 4000 scanner (Perkin Elmer), and image analysis and processing were performed using the ImaGene version 4.2 software package (BioDiscovery). The criteria for flagging spots were as follows: (i) empty-spot threshold of 2.0, (ii) poor-spot threshold of 0.4, and (iii) negative spots. Routinely over 80% of all spots passed these quality criteria. Raw data were stored in BASE (48). Flagged data were discarded, and the remaining, high-quality spot data were normalized using a LOWESS fit on M-A transformed data (64). To calculate a regulatory ratio for each gene, as far as the genes were represented by clones on the microarray, a weighted average of the M values of all clones that overlapped with the gene of interest was calculated. The weight used for each clone was equal to

the square of the overlap between the gene and clone divided by the total length of the gene. Consequently, this method weighs small overlapping fragments in lower proportions than those of larger overlapping fragments. Statistical analysis was performed with the statistical software program R (19) using the analysis of variance (ANOVA) model-fitting package *maanova* (24). Significant effects due to mutation (two levels), growth phase (three levels), and experiment (two levels) and their interactions were observed at different levels of significance ($P < 0.05$ and $P < 0.01$). Clones displaying these effects were selected and analyzed with the Eisen CLUSTER program (<http://rana.lbl.gov/EisenSoftware.htm>). Hierarchical clustering was performed using average linkage clustering and clustered genes were visualized with the Eisen Treeview program (<http://rana.lbl.gov/EisenSoftware.htm>).

Scanning electron microscopy. Wild-type and *lamA* mutant cultures were grown for 24 or 48 h in 24-well plates with 8-mm-diameter glass slides (Menzel-Glaser) on the bottom before sample preparation. Nucleopore polycarbonate membranes (Costar, Cambridge, Mass.) with 1- μ m pores were incubated for 30 min in a 0.01% poly-L-lysine solution in 0.1 M Tris-HCl buffer. Planktonic cells were spotted onto poly-L-lysine-coated polycarbonate membranes, and glass-adhered cells were treated as such on the glass slides. Bacteria were fixed for 30 min in 3% glutaraldehyde, and the membranes and glass slides were washed three times with deionized water, dehydrated with ethanol, using 30%, 50%, 70%, 90%, and finally 3 \times 100% ethanol and critical point dried by the CO₂ method (Balzers CPD 020; Balzers Union, Liechtenstein). Dried membranes and glass slides were mounted on sample holders by carbon adhesive tabs (Electron Microscopy Sciences, Washington, Pa.). Sample holders were positioned inside a sputter coater (JEOL JFS 1200 fine coater), and samples were sputter coated with 10-nm gold and analyzed in a scanning electron microscope (JEOL JSM-5600 LV) at 3 kV. Images were recorded digitally.

Overexpression of LamBD using the nisin-controlled expression (NICE) system. The *lamBD* genes were amplified by PCR with primers LamBD-NICE-NcoI with LamBD-NICE-KpnI and proofreading Platinum Pfx DNA polymerase (Invitrogen), using *L. plantarum* WCFS1 genomic DNA as a template. The PCR product was translationally fused (NcoI-KpnI) to the NICE vector pNZ8048 (9, 41) after the primers and vector were digested with NcoI and KpnI and cloned into the intermediate host *E. coli* JM109 by heat shock transformation. This plasmid, designated pNICE011, was subsequently cloned by electroporation into *L. plantarum* NCIMB8826 Int-1, carrying chromosomal integrations of the genes for the nisin response regulator *nisR* and histidine kinase *nisK* (41). Transformants were selected on MRS agar containing 5 μ g ml⁻¹ erythromycin and 10 μ g ml⁻¹ chloramphenicol and analyzed by colony PCR using pNZ8048 primers flanking the multiple cloning site, pNZ8048-F and pNZ8048-R. The NCIMB8826 Int-1 strain carrying pNICE011 was designated MSI011, and the strain carrying the empty vector pNZ8048 was designated MSI8048.

Strain MSI011 was grown to an OD₆₀₀ of 3.0 in a chemically defined medium (CDM) supplemented with 1% glucose and 10 μ g ml⁻¹ chloramphenicol (25). CDM was used to reduce the amounts of interfering proteinaceous impurities to improve analysis of overproduced peptides. The culture was 1:20 diluted to an OD₆₀₀ of 0.15 in 10 ml fresh CDM containing 5 μ g ml⁻¹ chloramphenicol and incubated for 3 h at 37°C. Nisin (ICN Biomedicals) was added to final concentrations of 0, 1.0, 5.0, 10.0, 20, or 60 ng ml⁻¹, and the cultures were incubated for another 3 h at 37°C.

LC/MS analysis of culture supernatant. Culture supernatants were prepared by centrifugation of cultures for 15 min at 6,500 \times g at 4°C. The supernatants were loaded onto a Sep-pak C₁₈ cartridge column (100 mg; Waters Co., Milford, Mass.), washed with 10 ml of 10% acetonitrile containing 0.1% trifluoroacetic acid (TFA) and eluted with 5 ml of 60% acetonitrile containing 0.1% TFA. Eluates were dried by evaporation using a Speedvac concentrator and redissolved in 160 μ l of 10% acetonitrile containing 0.05% TFA, and 80- μ l samples of these solutions were injected into a LC/MS device (LC, Agilent HP1100; column, Agilent Zorbax Eclipse XDB-C18, [2.1 \times 50 mm]; MS, JEOL Accutof T100LC [JEOL, Tokyo, Japan]). The column was eluted at a flow rate of 0.2 ml/min at 30°C with a linear gradient of acetonitrile (10% to 36% in 40 min) in 0.05% TFA aqueous solution. The column eluates were directly loaded into the electrospray ionization-time of flight mass spectrometer. Mass analyses were performed under the following conditions: positive polarity, capillary temperature 250°C, needle voltage of 2.0 kV, orifice voltage of 75 V for strain MSI011 or 35 V for the WCFS1 wild-type and MS Δ lamA strains, and ring lens voltage of 15 V. After scanning for molecular ions derived from column eluates in the *m/z* range of 100 to 2,000, extracted ion chromatograms were plotted with detector counts at the indicated *m/z*, with a window of one mass unit.

Chemical analysis of LamD558. LamD558 was purified from the Sep-pak-purified culture supernatants of strain MSI011 by the same LC device used for the LC/MS analysis described above. Amino acid sequence analysis was per-

formed with the purified LamD558 (0.5 μ g) by a peptide sequencer (Shimadzu PSQ-21). For alkaline hydrolysis, 10 μ l of 1 M KOH was added to the purified LamD558 (0.25 μ g/90 μ l of 10% acetonitrile containing 0.05% TFA) and incubated overnight at 37°C. Subsequently, 5 μ l of acetic acid was added to neutralize the reaction solution. Of this solution, 50 μ l was subjected to LC/MS, for which the same conditions were used as for the analysis of culture supernatant described above, except that the collision-induced dissociation (CID) spectrum was measured at the orifice voltage of 95 V. As a control, the synthetic linear 5-amino-acid peptide, Cys-Val-Gly-Ile-Trp, was subjected to the same LC/CID-MS analysis (see below).

Chemical synthesis of LamD558. The linear peptide Cys-Gly-Val-Ile-Trp was manually synthesized by the solid-phase method using the 9-fluorenylmethoxy carbonyl (Fmoc) strategy as previously described (35). *N*- α -Fmoc-S-trityl-L-cysteine (Novabiochem, Merck Limited, Tokyo, Japan) was used for synthesis of the protected peptide, and deblocking was done by stirring the resin carrying the synthetic peptide in a TFA-phenol-H₂O-ethanedithiol-trisopropylsilane mixture (86:5:5:3:1) for 1.5 h at room temperature. Two milligrams of the crude peptide was dissolved in 0.8 ml of *N,N*-dimethylacetamide, and (benzotriazole-1-yl)oxy-tris(pyrrolidino)phosphonium hexafluorophosphate (PyBop) (Novabiochem; 4 mg) and dimethylaminopyridine (4 mg) were added to the solution. The reaction mixture was stirred at room temperature for 6 h under N₂ gas and then added to 32 ml of ice-cold water. The solution was loaded onto a Sep-pak C₁₈ cartridge column (Waters; 1 ml), the column was washed with 10 ml of 15% acetonitrile containing 0.1% TFA, and the cyclized peptide was eluted with 5 ml of 60% acetonitrile containing 0.1% TFA. The obtained peptide was further purified by reverse-phase high-performance liquid chromatography (HPLC) using a linear gradient of acetonitrile in 0.1% TFA on a Pegasil octyldecyl silane column (0.46 \times 15 cm; Senshu Kagaku, Tokyo, Japan).

Real-time RT-PCR. A small number of open reading frames (ORFs) was chosen for quantitative real-time reverse transcription-PCR (RT-PCR) confirmation of data obtained from microarray analysis at early, mid-, and late logarithmic growth phases, as described above. To analyze the functionality of LamD558, synthetic peptide was added at 100 and 500 nM to early-log-phase wild-type cultures (OD₆₀₀ of 0.5) and RNA was isolated at 0.5, 1.0, and 2.0 h postinduction, as described above. Induction of gene expression of selected ORFs was determined by real-time RT-PCR quantification. cDNA was generated from total RNA after reverse transcription with random hexamers, according to the manufacturer's instructions (Invitrogen). Real-time PCR was performed on cDNA using gene-specific primers (Table 2) with the Bio-Rad SYBR Green kit in a Bio-Rad I-Cycler. Measurements were performed in triplicate, and the gene-specific mRNA amount was normalized against the 16S rRNA amount in the sample.

RESULTS

***lamBDCA* operon of *L. plantarum*.** The *L. plantarum* WCFS1 genome encodes a two-component regulatory system that is homologous to the *agr* system of *S. aureus* and was therefore designated *lam* for *Lactobacillus agr*-like module (lp_3580 to lp_3582 on the *L. plantarum* WCFS1 genome project website (<http://www.cmbi.kun.nl/lactobacillus>) (27). The *lamBDCA* genes (Fig. 1A) are predicted to code for a histidine protein kinase LamC, showing 24% identity to the *S. aureus* AgrC protein, and its cognate response regulator LamA showing 37% identity to the *S. aureus* AgrA protein. It is also predicted to encode LamB, a protein showing 30% identity to the *S. aureus* AgrD-processing protein AgrB. Alignment of the putative *lamD*-encoded peptide (*lamD* gene located between the *lamB* and *lamC* genes) with staphylococcal AgrD peptide sequences showed that it contained the conserved amino acids found in AgrD peptides (Fig. 1B). The *lamD* gene therefore appeared to encode an AIP precursor. The amino acids shown in bold type in Fig. 1B (LVMCCVGIW) were predicted to comprise the AIP sequence that could be cleaved from the precursor peptide LamD and modified to a cyclic thiolactone peptide, in analogy with the *agr* and *fsr* systems in staphylococci (20, 40) and *E. faecalis*, respectively (34). The expression of

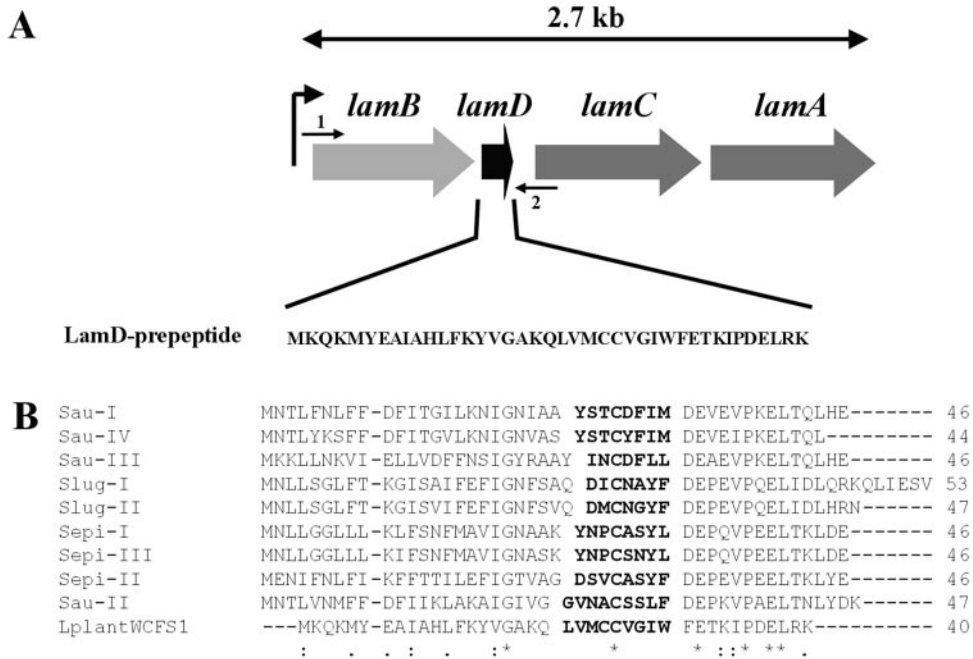


FIG. 1. (A) Schematic representation of the gene organization of the *lamBDCA* operon, as deduced from the *Lactobacillus plantarum* WCFS1 genome project (<http://www.cmbi.kun.nl/lactobacillus>). The position and direction of NICE cloning primer LamBD-NICE-NcoI (arrow 1) and NICE cloning primer LamBD-NICE-KpnI (arrow 2) are shown. (B) Alignment of the *L. plantarum* WCFS1 LamD prepeptide with staphylococcal AgrD prepeptide sequences. The numbers of amino acids in the prepeptides are shown to the right of the sequences. Sau-I to -IV, *S. aureus* pherotypes I to IV; Slug-I and -II, *Staphylococcus lugdunensis* pherotypes I and II; Sepi-I to -III, *S. epidermidis* pherotypes I to III; LplantWCFS1, *L. plantarum* WCFS1. Amino acids of determined or predicted AIP sequences are shown in bold type. Asterisks indicate conserved amino acids in all sequences, colons indicate conserved amino acid substitutions, and dots indicate semiconserved amino acid substitutions according to physicochemical criteria. Gaps introduced to maximize alignment are indicated by dashes.

lamBDCA during growth was analyzed by Northern blot analysis and appeared to be expressed as a single 2.7-kb transcript, comprising the complete *lamBDCA* operon. Expression was detectable at lower levels in early growth phases with a clear 2.5- to 3.0-fold increase at 5 h postinoculation (mid-exponential phase) that appeared to be maintained until late log and early stationary phase (Fig. 2), suggesting growth phase-dependent transcription regulation.

Effect of *lamA* deletion on adherence. A *lamA* gene replacement mutant was constructed, as deletion of this regulator should exclude cross talk to the *lam* system by other regulatory circuits. Initial experiments showed no differences in growth rate and cell or colony morphology between the wild type and the *lamA* mutant (data not shown). As *agr* systems in staphylococci are involved in biofilm formation (65), the ability to adhere to different surfaces as well as cell-cell aggregation was investigated for the wild type and the *lamA* mutant. Both the wild type and the *lamA* mutant did not form planktonic cell aggregates or adhere to polystyrene (data not shown). However, the mutant showed significantly decreased glass adherence compared to the wild type after both 24 and 48 h, as determined in a quantitative assay ($P < 0.001$; Fig. 3). Scanning electron microscopy analysis of the wild type and the *lamA* mutant confirmed that the mutant did not form a distinct biofilm on glass slides in contrast to the wild type. The wild type formed a dense layer with protruding structures, while the mutant formed only a thin layer on the slides (Fig. 4). The cell

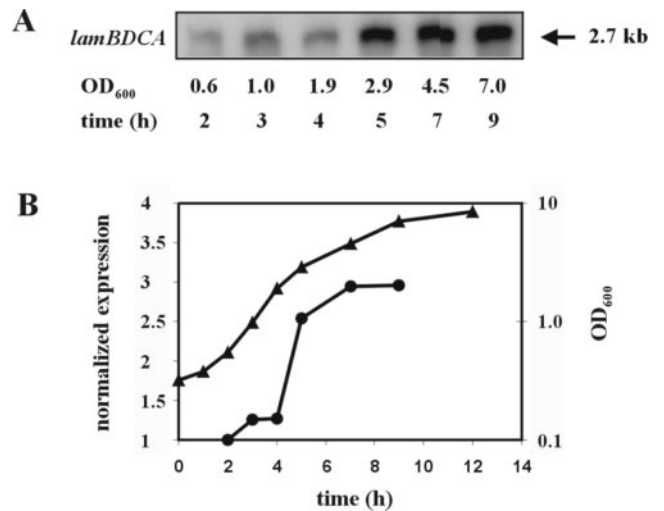


FIG. 2. Northern blot analysis of temporal expression of the *lam* cluster. (A) Expression of *lam* during growth using a *lamC* internal probe. Similar results were obtained with either the *lamB* or *lamA* probe. (B) Graphical representation of *lam* expression levels on Northern blots normalized against the 16S rRNA expression level. Symbols: triangles, OD₆₀₀ of MRS culture; circles, normalized *lam* expression.

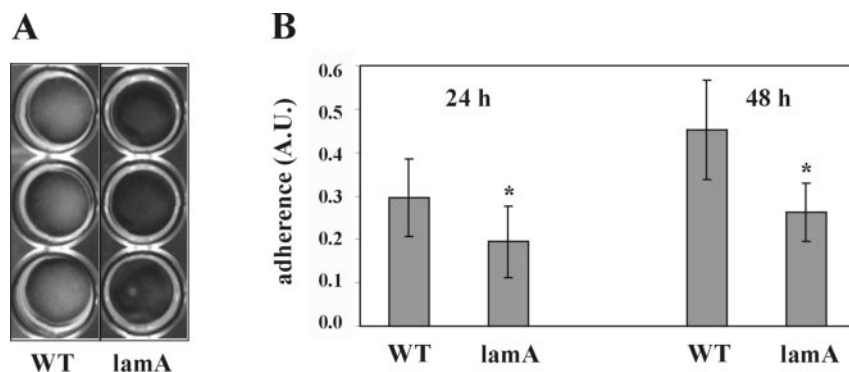


FIG. 3. Quantification of glass adherence in 24-well plates of the *L. plantarum* WCFS1 wild-type (WT) and Δ lamA (*lamA*) strains grown in MRS. (A) Picture showing glass-adhered cells grown in MRS in 24-well plates with glass cover slides after the phosphate-buffered saline wash step. (B) Quantification of crystal violet-stained glass-adhered cells in 24-well plate assay. Adherence of wild-type (WT) and Δ lamA (*lamA*) strains was measured in arbitrary units (A.U.). Means \pm standard errors (error bars) of three 24-well plates, with six wells measured per plate are shown. Values that were statistically significant different from the WT value ($P < 0.001$) are indicated by an asterisk. Statistical comparisons were done using the Student's *t* test (two-tailed, two-sample equal variance).

surfaces of both strains showed no visible differences at higher magnifications (data not shown).

DNA microarray transcriptional analysis of the *lamA* mutant versus the wild type. To study the global effects of the *lamA* deletion, transcription profiles in early, mid-, and late

logarithmic growth phases (OD_{600} s of 0.6, 2.0, and 4.8, respectively) were determined for the wild-type and *lamA* mutant strains, using a clone-based microarray. After the slides were scanned, clones showing significant differences in gene expression for the mutation effect were selected using ANOVA statistical analysis and their transcription profiles were hierarchically clustered. Clones displaying a significant mutation effect ($P < 0.05$) independently and consistently identified several genes with a difference in expression profile for the *lamA* mutant compared to the wild type (Table 3). Hierarchical cluster analysis of the transcription profiles per clone identified four distinct clusters of responding genes (Table 3). Cluster 1 contained several sugar utilization genes that were strongly down-regulated in late logarithmic phase only (e.g., sucrose, cellobiose, and trehalose phosphotransferase system genes lp_0185, lp_0436, and lp_0264, respectively). Cluster 2 encompassed constitutively down-regulated genes, with the highest effect in mid-logarithmic growth phase, coding for the *lamB-DCA* locus (lp_3580 to lp_3582) and several flanking genes as well as genes encoding integral membrane proteins (e.g., lp_0926, lp_3575, and lp_3577). Cluster 3 encompassed constitutively up-regulated genes, with the highest effect in early logarithmic growth phase, coding for a complete surface polysaccharide locus (*cps2*, lp_1197 to lp_1211). Finally, cluster 4 contained genes that mainly showed up-regulation in mid-logarithmic phase, with most gene functions related to pyrimidine biosynthesis (lp_2698 to lp_2703). The results obtained by microarray analysis were confirmed by quantitative real-time RT-PCR, using gene-specific primers for gene *lamC* (lp_3581) and ORFs lp_1197 and lp_1204 for *cps2* (Table 3).

Overexpression of LamBD using the NICE system. To confirm the presence and elucidate the chemical structure of the predicted AgrD-like peptide, the *lamBD* genes were overexpressed in *L. plantarum* NCIMB8826 Int-1 using the NICE overproduction system (41). Overexpression was induced, and culture supernatants were analyzed by LC/MS analysis. Molecules eluted from a reverse-phase column were traced in the extracted ion chromatograms at the protonated molecular masses of possible LamD-derived peptide candidates. These

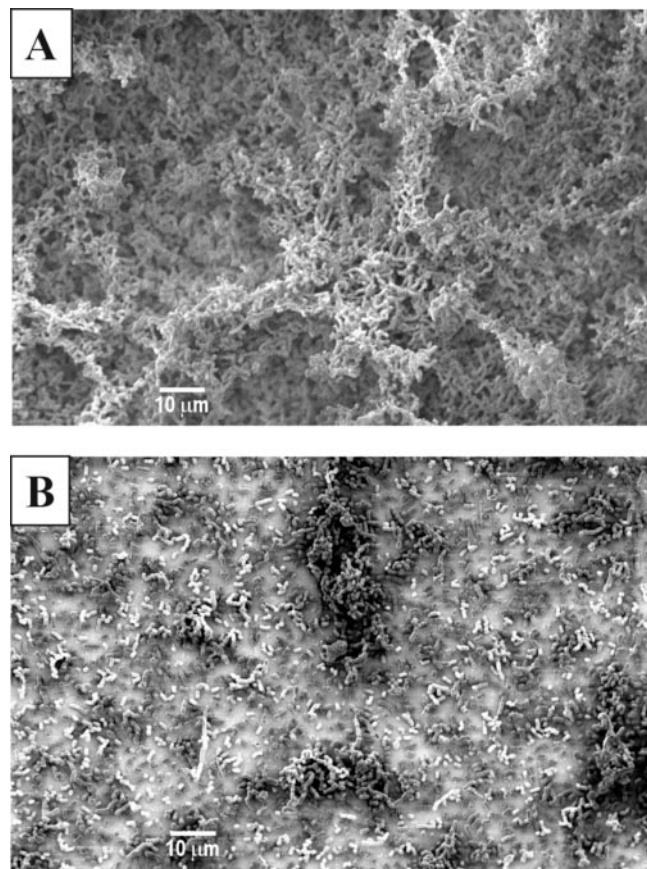


FIG. 4. Scanning electron micrographs of biofilm structures of glass-adhered cells of the wild type (A) and *lamA* mutant (B). Magnification, $\times 1,000$.

TABLE 3. Hierarchical clusters of genes showing significant differences in gene expression after ANOVA statistical analysis in the *lamA* mutant versus wild-type strain during early, mid-, and late logarithmic growth

Cluster and ORF ^a	Gene ^b	Description	No. of clones	Change (fold) ^c		
				E	M ^d	L
Cluster 1						
lp_0184	<i>sacK1</i>	Fructokinase	2	1.1	0.0	-12.1
lp_0185	<i>ptsIBC<i>A</i></i>	Sucrose PTS, EIIBCA ^e	3	1.0	-0.2	-13.6
lp_0187	<i>sacA</i>	β-Fructofuranosidase	1	1.1	-0.3	-18.5
lp_0188	<i>sacR</i>	Sucrose operon repressor	1	0.3	1.6	-14.6
lp_0189	<i>agl2</i>	α-Glucosidase	1	0.3	1.6	-14.6
lp_0263	<i>treA</i>	α,α-Phosphotrehalase	1	-2.2	0.4	-15.3
lp_0264	<i>pts4ABC</i>	PTS, trehalose-specific IIBC component	2	-1.9	0.4	-13.9
lp_0435		Transcription regulator, GntR family	1	1.8	0.4	-8.2
lp_0436	<i>pts7C</i>	Cellobiose PTS, EIIC	1	1.8	0.4	-8.2
lp_3480	<i>galT</i>	UTP-hexose-1-phosphate uridylyltransferase	1	1.1	1.4	-10.6
lp_3481	<i>galE4</i>	UDP-glucose 4-epimerase	1	1.1	1.4	-10.6
lp_3482	<i>galK</i>	Galactokinase	1	1.4	-0.2	-21.9
Cluster 2						
lp_0525	<i>kup1</i>	Potassium uptake protein	1	-2.8	-3.9	-2.7
lp_0526	<i>carB</i>	Carbamoyl-phosphate synthase, large subunit	1	-2.8	-3.9	-2.7
lp_0683		Prophage P1 protein 60	1	0.5	-4.5	-3.7
lp_0684		Prophage P1 protein 61	1	0.5	-4.5	-3.7
lp_0925		Acyltransferase	1	-0.7	-4	-5.7
lp_0926		Integral membrane protein	1	-8.8	-11	-6.1
lp_0927		Hypothetical protein	2	-8.0	-10.4	-6.7
lp_0928		Hypothetical protein	2	-8.0	-10.4	-6.7
lp_0929	<i>asp1</i>	Alkaline shock protein	2	-8.0	-10.4	-6.7
lp_0930	<i>asp2</i>	Alkaline shock protein	2	-8.0	-10.4	-6.7
lp_0931	<i>hpaG</i>	2-Hydroxyhepta-2,4-diene-1,7-dioate isomerase/5-carboxymethyl-2-oxo-hex-3-ene-1,7-dioatedecarboxylase (putative)	1	-7.1	-9.8	-7.3
lp_2658		Glycosyltransferase (putative)	2	-4.5	-3.8	-3.2
lp_2743		ABC transporter, ATP-binding protein	1	-7.6	-10.5	-8
lp_2744		ABC transporter, permease protein	1	-7.6	-10.5	-8
lp_3045		Short-chain dehydrogenase/oxidoreductase	1	-6.6	-4.8	-3.1
lp_3047		Hypothetical protein	1	-6.6	-4.8	-3.1
lp_3575		Integral membrane protein	1	-6.7	-11	-7.5
lp_3577		Integral membrane protein	2	-4.6	-3.8	-3.7
lp_3578	<i>kat</i>	Catalase	4	-4.4	-3.8	-3.6
lp_3580	<i>lamA</i>	Response regulator; homologue of accessory gene Regulator protein A	3	-2.7	-4.7	-2.8
lp_3581	<i>lamC</i>	Histidine protein kinase; sensor protein	3	-2.7 (-2.3)	-4.7 (-2.8)	-2.8 (-2.7)
lp_3581a	<i>lamD</i>	Homologue of accessory gene regulator protein D, peptide pheromone precursor	1	-2.4	-4.7	-2.7
lp_3582	<i>lamB</i>	Homologue of accessory gene regulator protein B	1	-2.4	-4.7	-2.7
lp_3583	<i>clpL</i>	ATP-dependent Clp protease, ATP-binding subunit ClpL	3	-21.6	-27.6	-11.7
lp_3586	<i>lox</i>	Lactate oxidase	2	-24.5	-28.7	-22.7
Cluster 3						
lp_1197	<i>cps2A</i>	Exopolysaccharide biosynthesis protein	1	40.5 (21.7)	16.6 (9.9)	19.0 (21.7)
lp_1198	<i>cps2B</i>	Exopolysaccharide biosynthesis protein; chain length determinant Wzz	2	28.9	16.6	16.1
lp_1199	<i>cps2C</i>	Exopolysaccharide biosynthesis protein	1	17.2	16.5	13.2
lp_1200	<i>galE2</i>	UDP-glucose 4-epimerase	3	26.6	14.3	18.5
lp_1201	<i>cps2E</i>	Priming glycosyltransferase	3	26.6	14.3	18.5
lp_1202	<i>cps2F</i>	Glycosyltransferase	2	37.0	12.5	13.3
lp_1203	<i>cps2G</i>	Glycosyltransferase	2	38.5	11.1	11.3
lp_1204	<i>cps2H</i>	Polysaccharide polymerase	2	28 (37)	7.8 (10.4)	8.1 (12.4)
lp_1205	<i>cps2I</i>	Repeat unit transporter	3	19.2	3.7	4.4
lp_1206	<i>cps2J</i>	Glycosyltransferase	1	18	2.6	3.6
lp_1207		Hypothetical protein	1	11.6	1.9	3.4
lp_1208		Hypothetical protein	1	11.6	1.9	3.4
lp_1210		Hypothetical protein	1	5.5	0.7	1.3
lp_1211		Hypothetical protein	1	5.5	0.7	1.3
Cluster 4						
lp_0254	<i>cysE</i>	Serine O-acetyltransferase	2	-0.1	5.5	5.4
lp_0255	<i>metC1</i>	Cystathionine β-lyase	3	-0.4	5.8	5.4

Continued on facing page

TABLE 3—Continued

Cluster and ORF ^a	Gene ^b	Description	No. of clones	Change (fold) ^c		
				E	M ^d	L
lp_0256	cysK	Cysteine synthase	2	-0.6	5.9	5.7
lp_2371	pyrP	Uracil transport protein	1	0.6	13.2	0.7
lp_2684	araT2	Aromatic amino acid-specific aminotransferase	2	0.6	0.8	19
lp_2685	dapA2	Dihydrodipicolinate synthase	2	0.6	0.8	19
lp_2698	pyrF	Orotidine-5'-phosphate decarboxylase	1	-0.4	34.6	-0.7
lp_2699	pyrD	Dihydroorotate oxidase	2	-0.6	46.6	-0.7
lp_2700	pyrAB	Carbamoyl-phosphate synthase, pyrimidine specific, large chain	4	0	59.2	-0.4
lp_2701	pyrAA	Carbamoyl-phosphate synthase, pyrimidine specific, small chain	4	0.6	69.9	-0.2
lp_2702	pyrC	Dihydroorotase	3	1	67.1	-0.3
lp_2703	pyrB	Aspartate carbamoyltransferase	1	1	11.3	0
lp_2704	pyrR1	Pyrimidine operon regulator	1	1	11.3	0

^a Gene lp_ number from the *Lactobacillus plantarum* WCFS1 genome project (<http://www.cmbi.kun.nl/lactobacillus>).

^b Previously reported gene name.

^c Average change in the *lamA* mutant versus the wild-type strain during early (E), mid- (M), and late (L) logarithmic growth. Average of four arrays unless specified otherwise. Average of all significant clones encoding the gene. The values in parentheses are the fold changes determined by real-time RT-PCR.

^d Average of three arrays instead of four arrays.

^e PTS, phosphotransferase system; EIIBCA, enzyme IIBCA.

candidates were predicted to be thiolactone peptides of 5 to 10 residues within the amino acid stretch running from Leu-21 to Phe-30 of the LamD precursor peptide sequence on the basis of the alignments with staphylococcal AgrD precursor peptides (Fig. 1B). Among those mass chromatograms, only one at a m/z value of 559 showed a clear peak at a retention time of 27 min in the detected ion count, which suggested the presence of a five-residue thiolactone peptide from Cys-25 to Trp-29 (sequence CVGIW; Fig. 5A). Compared to the mass chromatogram of a noninduced culture supernatant, this peak clearly increased with increasing amounts of nisin (Fig. 5B). The peptide contained in this peak was designated LamD558 on the basis of its molecular mass. The HPLC fraction corresponding to this peak was collected and subjected to N-terminal amino acid sequencing on an automated peptide sequencer. This yielded the peptide sequence X-Val-Gly-Ile-X, which was in agreement with the proposed thiolactone structure in which Cys-1 was linked to Trp-5 via a thioester bond. The determined accurate mass for this peptide was a m/z value of 559.2704, which was identical to the M+H value of 559.2703 that was calculated from the molecular formula of the predicted thiolactone peptide CVGIW. Alkaline treatment of LamD558 increased the molecular weight by 18 mass units, suggesting that the thiolactone peptide was linearized by hydrolysis of the thioester bond (data not shown). CID MS of the alkaline-treated LamD558 produced fragment ions at m/z values of 260, 345, and 373, each corresponding to b3, a4, and b4 ions of the deduced peptide CVGIW, and the fragmentation pattern was identical to that of the chemically synthesized five-residue linear peptide CVGIW (Fig. 6). Finally, we confirmed that the synthetic peptide possessing the proposed structure showed the same retention time in reverse-phase HPLC as LamD558 did (Fig. 7). From these results, we conclude that *lamD* encodes a five-residue thiolactone peptide with the sequence CVGIW, which matches the predicted *lamD* precursor peptide sequence (Fig. 1 and 8).

LamD558 could also be detected by LC/MS analysis in culture supernatants of the wild-type strain as a function of time

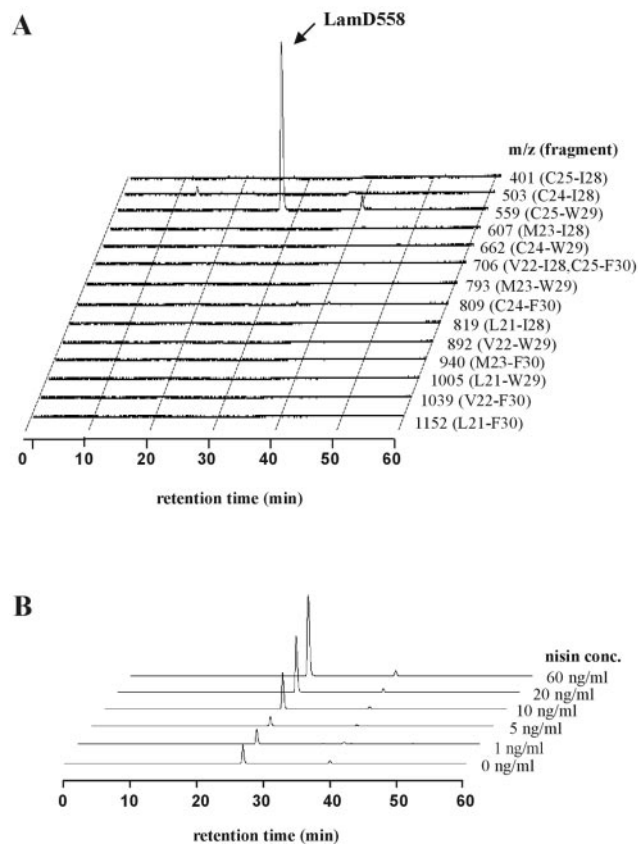


FIG. 5. LC/MS analysis of culture supernatant of strain MSI011. The culture supernatant was prepared and analyzed by LC/MS as described in Materials and Methods. (A) Three-dimensional view of extracted ion chromatograms at different m/z values corresponding to possible LamD-derived peptide candidates. Twenty nanograms of nisin per milliliter was used for induction. Each m/z value used in the extracted ion chromatogram corresponds to a thiolactone peptide derived from the LamD fragment indicated in parentheses. (B) Three-dimensional view of extracted ion chromatograms at a m/z value of 559 (C25-W29) with increasing concentrations (conc.) of nisin added as indicated.

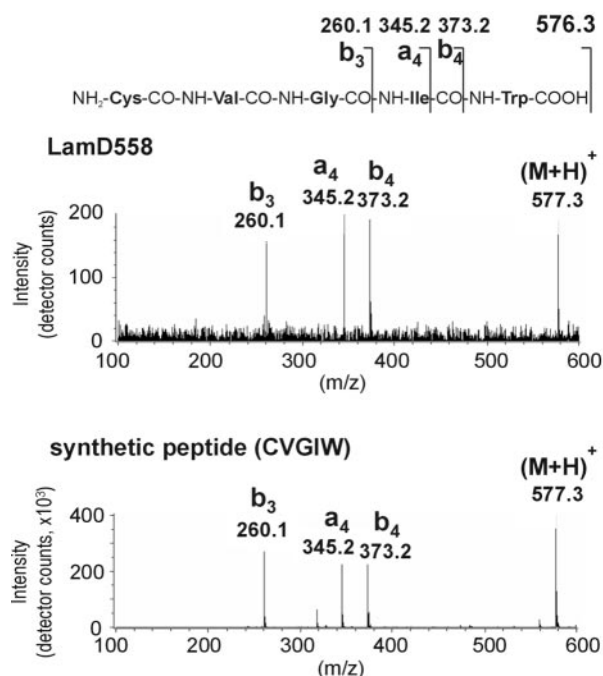


FIG. 6. Collision-induced dissociation mass spectra of alkaline-treated LamD558 (top) and the synthetic linear CVGIW peptide (bottom). The alkaline-treated LamD558 and the synthetic pentapeptide were subjected to the LC/CID-MS analysis as described in Materials and Methods.

(Fig. 9). The amount of LamD558 increased markedly between 3 and 9 h postinoculation, corresponding to the mid-log to late log growth phase. In a *lamA* deletion strain, the amount of LamD558 detected was several times lower than that of the

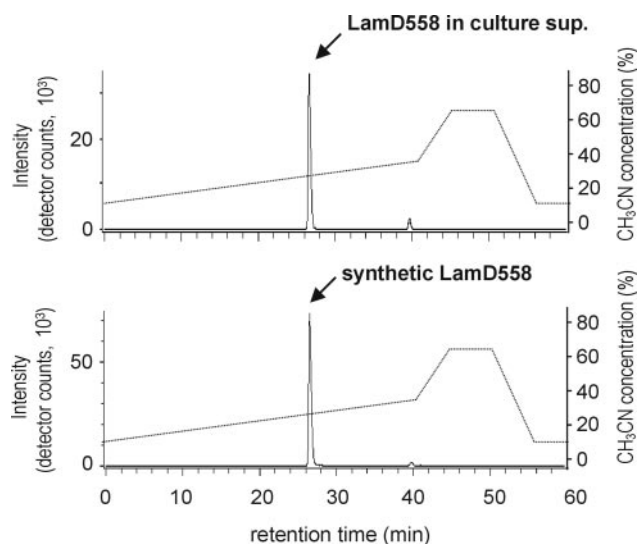


FIG. 7. LC/MS analysis of LamD558 in culture supernatant (sup.) of strain MS1011 (top) and chemically synthesized LamD558 (bottom). The extracted ion chromatogram at a *m/z* value of 559 was displayed for each analysis. The culture supernatant was prepared, and LC/MS analysis was performed as described in the legend to Fig. 5A. The synthetic LamD558 was prepared as described in Materials and Methods.

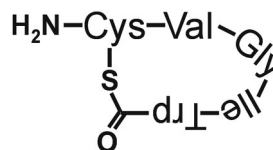


FIG. 8. Structure of peptide LamD558.

wild-type strain throughout the sampling period, which is in agreement with the autoregulatory function that was predicted for *lamBDCA* (Fig. 9).

Functionality of LamD558. To study the functionality of the identified LamD558 peptide, induction experiments were performed with early-log-phase wild-type cultures using synthetic LamD558 peptide. mRNA amounts for genes *lamC* (lp_3581) and lp_1204 were quantified using real-time RT-PCR at 0.5, 1.0, and 2.0 h postinduction. Induction with both 100 nM (concentration in mid-log-phase culture supernatants) and 500 nM LamD558 showed no autoinducing effect for *lamC* but showed instead a nonanticipated moderate decrease (decreases of 1.1- to -2.2-fold at 100 nM and of 2.6- to 1.9-fold at 500 nM). For gene lp_1204, a moderate decrease in gene expression was observed (decreases of 1.6- to 5.0-fold at 100 nM and of 4.8- to 2.3-fold at 500 nM), which was expected considering the microarray analysis that showed increased lp_1204 gene expression in the *lamA* mutant.

DISCUSSION

The function of an *agr*-like two-component regulatory system of *Lactobacillus plantarum* WCFS1, designated *lamBDCA*, was studied by mutation analysis and a global transcriptional profiling approach. The *lamBDCA* genes were expressed in all growth phases with a clear increase at 5 h postinoculation (mid-exponential phase) that remained until late log to stationary phase, suggesting growth phase-dependent transcrip-

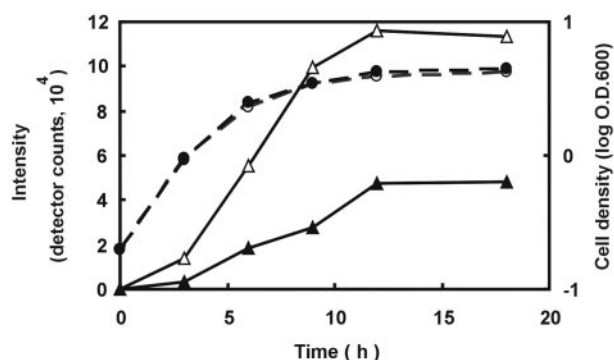


FIG. 9. Time course of LamD558 production in culture filtrates of wild-type and *lamA* mutant strains grown in CDM. Solid line shows LamD558 intensity (open triangle, wild-type strain; closed triangle, *lamA* mutant strain). Broken line shows the optical density of cultures at 600 nm (log O.D.₆₀₀) (open circle, wild-type strain; closed circle, *lamA* mutant strain). Culture filtrates were collected and analyzed by LC/MS. Overnight cultures were inoculated into CDM to an OD₆₀₀ of 0.15 and cultured at 30°C. Culture filtrates were collected at the indicated times and analyzed by LC/MS as described in Materials and Methods. The height of the LamD558 peak in each extracted ion chromatogram at a *m/z* value of 559 was plotted in the graph.

tion regulation. In analogy, analysis of the homologous *agr* and *fsr* systems from *S. aureus* and *E. faecalis* OG1RF, respectively, showed transcription initiation at mid- to late exponential growth phase (45, 56). A *lamA* mutant was constructed and showed decreased attachment in a glass adherence assay, which pointed to an involvement in regulation of cell surface properties. The *lamA* mutant and wild-type strains showed similar growth curves, which simplified global transcription analysis. Transcriptional profiling using microarrays showed an altered transcription profile of the *lamA* mutant compared to that of the wild-type strain for a limited number of loci, with several gene clusters showing continuous up- or down-regulation for all growth phases analyzed. The *lamBDCA* genes were continuously down-regulated in the *lamA* mutant, confirming its analogy with an *agr*-like autoinducing system. Many of the *lamA*-affected genes appeared to be involved in cell surface properties, such as the up-regulated surface polysaccharide biosynthesis genes and several down-regulated integral membrane proteins with unknown functions. Also UTP-hexose-1-phosphate uridylyltransferase, UDP-glucose-4-epimerase, and galactokinase, which are involved in the production of activated glucose and galactose (51, 63), were down-regulated in the *lamA* mutant, markedly in late log phase. This was also found for an *agr*-null mutant in *S. aureus* (12). Several pyrimidine biosynthesis genes, which might be linked to UTP biosynthesis from UMP (5), as well as an uracil transport protein, were up-regulated. The up-regulation of these genes could suggest increased cellular UTP levels that might be necessary for and directed to surface polysaccharide biosynthesis via (UDP)-glucose, as the pathway via (UDP)-galactose is down-regulated, while the surface polysaccharide biosynthesis genes are up-regulated (62). Finally, several genes mainly linked to sucrose, cellobiose, and trehalose uptake and fructose metabolism were down-regulated in late log phase, which might indicate that *lamA* regulates transport of these sugars. At this stage, it is not clear whether the responding genes are under direct regulation of *lamA* or are the result of secondary effects. The application of sequence pattern recognition software like MEME (3) did not allow the identification of specific conserved potential *cis*-acting elements in the upstream regions of the genes affected by the *lamA* mutation. This might suggest that the majority of the identified responses represent secondary regulatory effects rather than primary *lamA*-regulated effects. A similar response was found for an *agr*-null mutant in *S. aureus* (12).

The *lamA* deletion stimulates surface polysaccharide expression (up-regulation of *cps2*) in *L. plantarum* WCFS1, while it reduces adherence to a glass surface. At first glance, these findings may seem to contradict the results of other studies, which show that exopolysaccharide production is necessary for biofilm formation (53). Reports on *agr* systems in *S. aureus* and *Staphylococcus epidermidis* have suggested a positive influence of *agr* on biofilm formation (60, 61). However, recent studies by Yarwood et al. (65) indicate that depending on the environmental conditions, the biofilm development can either be inhibited or enhanced. This could indicate that other factors and regulatory systems might be involved in these phenotypes. If the surface polysaccharide operon codes for capsular (membrane-associated) rather than excreted exopolysaccharides, shielding of adhesion factors by capsular polysaccharides could

explain our findings. Such shielding has also been observed in *S. aureus* and might explain our observations, with respect to the reduced glass adherence of the *lamA* mutant (43). Finally, there are reports on surface characteristics being dependent on the relative levels of expression of different lipopolysaccharides in *Pseudomonas aeruginosa*, which influence adherence properties to hydrophilic and hydrophobic surfaces (31). The detectable production of a biofilm may therefore be due to a delicate balance between different polysaccharides produced by *L. plantarum*, keeping in mind that the *L. plantarum* genome contains four different surface polysaccharide gene clusters, *cps1* (lp_1176 to lp_1190), *cps2* (lp_1197 to lp_1211), *cps3* (lp_1215 to lp_1227), and *cps4* (lp_2099 to lp_2108) (27).

The number of ORFs showing altered gene expression in the *lamA* mutant was 65 out of 3,052 predicted ORFs (about 2%), which is lower than the 138 genes (about 5%) that were reported for an *agr*-null mutant in *S. aureus* (12). In that study, microarray comparison of the wild type versus an *agr*-null mutant in *S. aureus* showed that *agr* up-regulates *agrBDCA* and many recognized *agr* up-regulated genes coding for extracellular accessory proteins involved in virulence. In addition, several *agr*-regulated genes were identified, suggesting a coupling of the *agr* system to a global cellular response, such as the up-regulated pyrimidine biosynthesis genes (*pyrAA*, *pyrR*, *arcB*, and *arcS*) and the UTP-glucose-1-phosphate uridylyltransferase gene and down-regulated genes coding for alpha-glucosidase (*treA*) and a GntR-type transcriptional regulator (12). Strikingly, similar responding genes were also found for the nonpathogenic *L. plantarum* WCFS1 *lamA* mutant, suggesting that *agrBDCA* and *lamBDCA* might influence regulation of these genes via comparable molecular mechanisms (Table 3).

To identify the presence of a secreted *agr*-like AIP and elucidate its structure, homologous overexpression of the *lamBD* genes, using the NICE system, was combined with LC/MS analysis of culture supernatants. This strategy allowed for the detection of secreted peptides in culture supernatants as well as a direct MS identification strategy by multistage MS, which had proven to be successful for rapid detection of staphylococcal AIPs (23). *L. plantarum* strains carrying the *lamBD* overexpression construct under the control of an autoinducing promoter were cultured in chemically defined medium to reduce the amount of impurities that could generate high peptide background levels in chromatography and to reduce the ionization efficiency of the overexpressed target peptide during mass spectrometry. Using these methods, overexpression of the *lamBD* genes identified an overproduced *agr*-like peptide with the sequence CVGIW, which matched within the predicted LamD peptide, and contained a cyclic thiolactone bond from C to W (Fig. 1 and 8). This is analogous to structural data obtained for autoinducing peptides in staphylococci and is the first finding of an *agr*-like peptide in lactobacilli. LamD558 consists of a five-amino-acid ring similar to known staphylococcal autoinducing peptides, but it lacks the N-terminal tail moiety consisting of two to four amino acids that is found in staphylococcal AIPs (40). In staphylococci, this tail moiety is essential for functional interaction with the AgrC sensor (32). LamD558 is probably formed during processing and transport of the precursor peptide LamD by the AgrB-homologous protein LamB, although the mechanism has not yet been elucidated. A precursor peptide-processing mechanism has how-

ever been proposed for processing of AgrD by the AgrB protein in *S. aureus* (46) and GBAP by the FsrB protein in *E. faecalis* (37), involving a histidine and cysteine residue that are found to be conserved in all known AgrB homologues (37, 46). These residues are critical for processing of AgrD by AgrB and GBAP by FsrB and might also serve this function in LamB. During the course of the LC/MS analysis, two other nisin-induced substances were detected in the mass chromatograms at *m/z* values of 559 (small peak at retention time of 40 min in Fig. 5A) and 678 (peak at retention time 29 min) (data not shown). These two compounds may be by-products or precursors in the biosynthesis of LamD558. LamD558 was also detected in the extracted ion chromatograms of the wild-type strain. From the UV absorption at 280 nm of this peak, the concentration in the mid-log-phase culture supernatant was approximately 100 nM, which was several times higher than that of staphylococcal autoinducing peptides (30, 49). The LamD558 peak was also detected in culture supernatants of the *lamA* knockout strain. However, it was clearly decreased than that from the wild-type strain. These results suggest that the expression of the *lamBDCA* operon is positively regulated by the LamCA two-component regulatory system, but a certain level of this expression occurs independently of this regulatory system. The time course data of LamD558 production in CDM culture supernatants of the wild-type strain showed that production of LamD558 was strongly increased from mid- to late log phase, which coincides with increased *lamBDCA* gene expression from mid-log phase on, as observed by Northern hybridization analysis (see above). The *lam* system therefore appears to show growth phase-dependent gene expression, as expected from the gene annotation as an *agr*-like quorum-sensing system.

Finally, induction with the LamD-encoded peptide LamD558 confirmed that LamD558 influenced Ip_1204 gene expression as was observed using microarray analysis. However, it did not indicate an autoregulatory role of LamD558 in *lam* gene expression. It might be that the LamD558 structure that was determined is not the active autoinducing structure. In addition, it could be that other (competing) peptides or regulatory systems are involved in regulation of *lam* gene expression. Further experiments are necessary to elucidate the regulatory mechanisms involved.

In conclusion, this is the first complete *agr*-like TCS described in lactobacilli that encodes a cyclic thiolactone AIP. Complete *agrBDCA*-like systems have until now been detected in and described only for pathogenic bacteria, such as staphylococci (11), *E. faecalis* (36), and *Listeria monocytogenes* (2), that have invasive properties or otherwise interact with host cells (18, 52). In analogy, the *L. plantarum lamBDCA* system might play a role in commensal host-microbe interactions, considering the observed effects on the capacity of a *lamA* mutant to adhere to surfaces (10).

ACKNOWLEDGMENTS

We thank Jacqueline Donkers and Adriaan van Aelst for technical assistance with scanning electron microscopy, Frank Schuren and Ted van de Lende for help with the microarrays, and Neeli Willemsen for technical assistance in our laboratory.

This research was supported in part by The Netherlands Organization for Scientific Research (NWO) and by a grant from the Takeda Science Foundation in Japan.

REFERENCES

- Ahrne, S., S. Nobaek, B. Jeppsson, I. Adlerberth, A. E. Wold, and G. Molin. 1998. The normal *Lactobacillus* flora of healthy human rectal and oral mucosa. *J. Appl. Microbiol.* **85**:88–94.
- Autret, N., C. Raynaud, I. Dubail, P. Berche, and A. Charbit. 2003. Identification of the *agr* locus of *Listeria monocytogenes*: role in bacterial virulence. *Infect. Immun.* **71**:4463–4471.
- Bailey, T. L., and C. Elkan. 1995. The value of prior knowledge in discovering motifs with MEME. *Proc. Int. Conf. Intell. Syst. Mol. Biol.* **3**:21–29.
- Bernard, N., T. Ferain, D. Garmyn, P. Hols, and J. Delcour. 1991. Cloning of the D-lactate dehydrogenase gene from *Lactobacillus delbrueckii* subsp. *bulgaricus* by complementation in *Escherichia coli*. *FEBS Lett.* **290**:61–64.
- Bringel, F., and J. C. Hubert. 2003. Extent of genetic lesions of the arginine and pyrimidine biosynthetic pathways in *Lactobacillus plantarum*, *L. paraplantarum*, *L. pentosus*, and *L. casei*: prevalence of CO₂-dependent auxotrophs and characterization of deficient *arg* genes in *L. plantarum*. *Appl. Environ. Microbiol.* **69**:2674–2683.
- Bron, P. A. 2004. The molecular response of *Lactobacillus plantarum* to intestinal passage and conditions. Ph.D. thesis. Wageningen University, Wageningen, The Netherlands.
- Caplice, E., and G. F. Fitzgerald. 1999. Food fermentations: role of microorganisms in food production and preservation. *Int. J. Food Microbiol.* **50**:131–149.
- Cheng, Q., E. A. Campbell, A. M. Naughton, S. Johnson, and H. R. Masure. 1997. The *com* locus controls genetic transformation in *Streptococcus pneumoniae*. *Mol. Microbiol.* **23**:683–692.
- De Ruyter, P. G. G. A., O. P. Kuipers, and W. M. de Vos. 1996. Controlled gene expression systems for *Lactococcus lactis* with the food-grade inducer nisin. *Appl. Environ. Microbiol.* **62**:3662–3667.
- De Vos, W. M., P. A. Bron, and M. Kleerebezem. 2004. Post-genomics of lactic acid bacteria and other food-grade bacteria to discover gut functionality. *Curr. Opin. Biotechnol.* **15**:86–93.
- Dufour, P., S. Jarraud, F. Vandenesch, T. Greenland, R. P. Novick, M. Bes, J. Etienne, and G. Lina. 2002. High genetic variability of the *agr* locus in *Staphylococcus* species. *J. Bacteriol.* **184**:1180–1186.
- Dunman, P. M., E. Murphy, S. Haney, D. Palacios, G. Tucker-Kellog, S. Wu, E. L. Brown, R. J. Zagursky, D. Shlaes, and S. J. Projan. 2001. Transcription profiling-based identification of *Staphylococcus aureus* genes regulated by the *agr* and/or *sarA* loci. *J. Bacteriol.* **183**:7341–7353.
- Duran Quintana, M. C., P. Garcia Garcia, and A. Garrido Fernandez. 1999. Establishment of conditions for green table olive fermentation at low temperature. *Int. J. Food Microbiol.* **51**:133–143.
- Enan, G., A. A. el-Essawy, M. Uyttendaele, and J. Debevere. 1996. Antibacterial activity of *Lactobacillus plantarum* UG1 isolated from dry sausage: characterization, production and bactericidal action of plantaricin UG1. *Int. J. Food Microbiol.* **62**:3304–3309.
- Fuqua, W. C., S. C. Winans, and E. P. Greenberg. 1994. Quorum sensing in bacteria: the LuxR-LuxI family of cell density-responsive transcriptional regulators. *J. Bacteriol.* **176**:269–275.
- Hancock, L. E., and M. Perego. 2004. The *Enterococcus faecalis* *fsr* two-component system controls biofilm development through production of gelatinase. *J. Bacteriol.* **186**:5629–5639.
- Hayward, A. C., and G. H. G. Davis. 1956. The isolation and classification of *Lactobacillus* strains from Italian saliva samples. *Br. Dent. J.* **101**:2733–2741.
- Heyer, G., S. Saba, R. Adamo, W. Rush, G. Soong, A. Cheung, and A. Prince. 2002. *Staphylococcus aureus agr* and *sarA* functions are required for invasive infection but not inflammatory responses in the lung. *Infect. Immun.* **70**:127–133.
- Ihaka, R., and R. Gentleman. 1996. R: a language for data analysis and graphics. *J. Comput. Graph. Stat.* **5**:299–314.
- Ji, G., R. C. Beavis, and R. P. Novick. 1995. Cell density control of staphylococcal virulence mediated by an octapeptide pheromone. *Proc. Natl. Acad. Sci. USA* **92**:12055–12059.
- Ji, G., R. Beavis, and R. P. Novick. 1997. Bacterial interference caused by autoinducing peptide variants. *Science* **276**:2027–2030.
- Josson, K., T. Scheirlinck, F. Michiels, C. Platteeuw, P. Stanssens, H. Joos, P. Dhaese, M. Zabeau, and J. Mahillon. 1989. Characterization of a gram-positive broad-host-range plasmid isolated from *Lactobacillus hilgardii*. *Plasmid* **21**:9–20.
- Kalkum, M., G. L. Lyon, and B. T. Chait. 2003. Detection of secreted peptides by using hypothesis-driven multistage mass spectrometry. *Proc. Natl. Acad. Sci. USA* **100**:2795–2800.
- Kerr, M. K., M. Martin, and G. A. Churchill. 2000. Analysis of variance for gene expression microarray data. *J. Comput. Biol.* **7**:819–837.
- Kets, E. P. W., E. A. Galinski, and J. A. M. de Bont. 1994. Carnitine: a novel compatible solute in *Lactobacillus plantarum*. *Arch. Microbiol.* **162**:243–248.
- Kleerebezem, M., L. E. N. Quadri, O. P. Kuipers, and W. M. De Vos. 1997. Quorum sensing by peptide pheromones and two-component signal-transduction systems in Gram-positive bacteria. *Mol. Microbiol.* **24**:895–904.
- Kleerebezem, M., J. Boekhorst, R. van Kranenburg, D. Molenaar, O. P. Kuipers, R. Leer, R. Turchini, S. A. Peters, H. M. Sandbrink, M. W. E. J.

- Fiers, W. Stiekema, R. M. Klein Lankhorst, P. A. Bron, S. M. Hoffer, M. N. Nierop Groot, R. Kerkhoven, M. de Vries, B. Ursing, W. M. de Vos, and R. J. Siezen. 2003. Complete genome sequence of *Lactobacillus plantarum* WCFS1. Proc. Natl. Acad. Sci. USA **100**:1990–1995.
28. Kuipers, O. P., M. M. Beerthuyzen, R. J. Siezen, and W. M. de Vos. 1993. Characterization of the nisin gene cluster *nisABTCIPR* of *Lactococcus lactis*, requirement of expression of the *nisA* and *nisI* genes for development of immunity. Eur. J. Biochem. **216**:281–291.
29. Lazdunski, A. M., I. Ventre, and J. N. Sturgis. 2004. Regulatory circuits and communication in gram-negative bacteria. Nat. Rev. Microbiol. **2**:581–592.
30. Lyon, G. J., P. Mayville, T. W. Muir, and R. P. Novick. 2000. Rational design of a global inhibitor of the virulence response in *Staphylococcus aureus*, based in part on localization of the site of inhibition to the receptor-histidine kinase, AgrC. Proc. Natl. Acad. Sci. USA **97**:13330–13335.
31. Makin, S. A., and T. J. Beveridge. 1996. The influence of A-band and B-band lipopolysaccharide on the surface characteristics and adhesion of *Pseudomonas aeruginosa* to surfaces. Microbiology **142**:299–307.
32. Mayville, P., G. Ji, R. Beavis, H. Yang, M. Goger, R. Novick, and T. W. Muir. 1999. Structure-activity analysis of synthetic autoinducing thiolactone peptides from *Staphylococcus aureus* responsible for virulence. Proc. Natl. Acad. Sci. USA **96**:1218–1223.
33. Merritt, J., F. Qi, S. D. Goodman, M. H. Anderson, and W. Shi. 2003. Mutation of *luxS* affects biofilm formation in *Streptococcus mutans*. Infect. Immun. **71**:1972–1979.
34. Nakayama, J., Y. Cao, T. Horii, S. Sakuda, A. D. L. Akkermans, W. M. de Vos, and H. Nagasawa. 2001. Gelatinase biosynthesis-activating pheromone: a peptide lactone that mediates a quorum sensing in *Enterococcus faecalis*. Mol. Microbiol. **41**:145–154.
35. Nakayama, J., Y. Cao, T. Horii, S. Sakuda, and H. Nagasawa. 2001. Chemical synthesis and biological activity of the gelatinase biosynthesis-activating pheromone of *Enterococcus faecalis* and its analogs. Biosci. Biotechnol. Biochem. **65**:2322–2325.
36. Nakayama, J., R. Kariyama, and H. Kumon. 2002. Description of a 23.9-kilobase chromosomal deletion containing a region encoding *fsr* genes which mainly determines the gelatinase-negative phenotype of clinical isolates of *Enterococcus faecalis* in urine. Appl. Environ. Microbiol. **68**:3152–3155.
37. Nakayama, J., E. Azab, E. Tanaka, Y. Murakami, K. Nishiguchi, R. Kariyama, H. Kumon, and K. Sonomoto. 2004. Overexpression and site-directed mutagenesis of FsrB, the AgrB-family protein involved in biosynthesis of cyclic peptide quorum, GBAP, in *Enterococcus faecalis*, poster 63C. In ASM Conference on Cell-Cell Communication in Bacteria (2nd). American Society for Microbiology, Washington, D.C.
38. Nes, I. F., and V. G. H. Eijsink. 1999. Regulation of group II peptide bacteriocin synthesis by quorum-sensing mechanisms, p. 175–192. In G. M. Dunny and S. C. Winans (ed.), Cell-cell signaling in bacteria. American Society for Microbiology, Washington, D.C.
39. Novick, R. P. 1999. Regulation of pathogenicity in *Staphylococcus aureus* by a peptide-based density-sensing system, p. 129–146. In G. M. Dunny and S. C. Winans (ed.), Cell-cell signaling in bacteria. American Society for Microbiology, Washington, D.C.
40. Novick, R. P. 2003. Autoinduction and signal transduction in the regulation of staphylococcal virulence. Mol. Microbiol. **48**:1429–1449.
41. Pavan, S., P. Hols, J. Delcour, M. C. Geoffroy, C. Grangette, M. Kleerebezem, and A. Mercenier. 2000. Adaptation of the nisin-controlled expression system in *Lactobacillus plantarum*: a tool to study *in vivo* biological effects. Appl. Environ. Microbiol. **66**:4427–4432.
42. Pieterse, B., R. H. Jellema, and M. van der Werf. Unpublished data.
43. Pohlmann-Dietze, P., M. Ulrich, K. B. Kiser, G. Doring, J. C. Lee, J. M. Fournier, K. Botzenhart, and C. Wolz. 2000. Adherence of *Staphylococcus aureus* to endothelial cells: influence of capsular polysaccharides, global regulator *agr*, and bacterial growth phase. Infect. Immun. **68**:4865–4871.
44. Qin, X., K. V. Singh, G. M. Weinstock, and B. E. Murray. 2000. Effects of *Enterococcus faecalis* *fsr* genes on production of gelatinase and a serine protease and virulence. Infect. Immun. **68**:2579–2586.
45. Qin, X., K. V. Singh, G. M. Weinstock, and B. E. Murray. 2001. Characterization of *fsr*, a regulator controlling expression of gelatinase and serine protease in *Enterococcus faecalis* OG1RF. J. Bacteriol. **183**:3371–3382.
46. Qiu, R., W. Pei, L. Zhang, J. Lin, and G. Ji. 2005. Identification of the putative staphylococcal AgrB catalytic residues involving in the proteolytic cleavage of AgrD to generate autoinducing peptide. J. Biol. Chem. **280**:16695–16704.
47. Ross, R. P., S. Morgan, and C. Hill. 2002. Preservation and fermentation: past, present and future. Int. J. Food Microbiol. **79**:3–16.
48. Saal, L. H., C. Troein, J. Vallon-Christersson, S. Grubberger, A. Borg, and C. Peterson. 15 July 2002, posting date. BioArray Software Environment (BASE): a platform for comprehensive management and analysis of microarray data. Genome Biol. **3**:software0003.1–0003.6. [Online.] <http://genomebiology.com/2002/3/8/SOFTWARE/0003>.
49. Saenz, H. L., V. Augsburger, C. Vuong, R. W. Jack, F. Götz, and M. Otto. 2000. Inducible expression and cellular location of AgrB, a protein involved in the maturation of the staphylococcal quorum-sensing pheromone. Arch. Microbiol. **174**:452–455.
50. Sambrook, J., E. F. Fritsch, and T. Maniatis. 1989. Molecular cloning: a laboratory manual, 2nd ed. Cold Spring Harbor Laboratory Press, Cold Spring Harbor, N.Y.
51. Schulman, H., and E. P. Kennedy. 1977. Identification of UDP-glucose as an intermediate in the biosynthesis of the membrane-derived oligosaccharides of *Escherichia coli*. J. Biol. Chem. **252**:6299–6303.
52. Sifri, C. D., E. Mylonakis, K. V. Singh, X. Qin, D. A. Garsin, B. E. Murray, F. M. Ausubel, and S. B. Calderwood. 2002. Virulence effect of *Enterococcus faecalis* protease genes and the quorum-sensing locus *fsr* in *Caenorhabditis elegans* and mice. Infect. Immun. **70**:5647–5650.
53. Stoodley, P., K. Sauer, D. G. Davies, and J. W. Costerton. 2002. Biofilms as complex differentiated communities. Annu. Rev. Microbiol. **56**:187–209.
54. Sturme, M. H. J., M. Kleerebezem, J. Nakayama, A. D. L. Akkermans, E. E. Vaughan, and W. M. de Vos. 2002. Cell to cell communication by autoinducing peptides in gram-positive bacteria. Antonie Leeuwenhoek **81**:233–243.
55. Tortosa, P., and D. Dubnau. 1999. Competence for transformation: a matter of taste. Curr. Opin. Microbiol. **2**:588–592.
56. Vandenesch, F., J. Kornblum, and R. P. Novick. 1991. A temporal signal, independent of *agr*, is required for *hla* but not *spa* transcription in *Staphylococcus aureus*. J. Bacteriol. **173**:6313–6320.
57. van Kranenburg, R., J. D. Marugg, I. I. van Swam, N. J. Willem, and W. M. de Vos. 1997. Molecular characterization of the plasmid-encoded *eps* gene cluster essential for exopolysaccharide biosynthesis in *Lactococcus lactis*. Mol. Microbiol. **24**:387–397.
58. Vaughan, E. E., M. C. De Vries, E. G. Zoetendal, K. Ben-Amor, A. D. L. Akkermans, and W. M. deVos. 2002. The intestinal LABs. Antonie Leeuwenhoek **82**:341–352.
59. Vesa, T., P. Pochart, and P. Marteau. 2000. Pharmacokinetics of *Lactobacillus plantarum* NCIMB8826, *Lactobacillus fermentum* KLD, and *Lactococcus lactis* MG1363 in the human gastrointestinal tract. Aliment. Pharmacol. Ther. **14**:823–828.
60. Vuong, C., H. L. Saenz, F. Gotz, and M. Otto. 2000. Impact of the *agr* quorum-sensing system on adherence to polystyrene in *Staphylococcus aureus*. J. Infect. Dis. **182**:1688–1693.
61. Vuong, C., C. Gerke, G. A. Somerville, E. R. Fischer, and M. Otto. 2003. Quorum-sensing control of biofilm factors in *Staphylococcus epidermidis*. J. Infect. Dis. **188**:706–718.
62. Welman, A. D., and I. S. Maddox. 2003. Exopolysaccharides from lactic acid bacteria: perspectives and challenges. Trends Biotechnol. **21**:269–274.
63. Yamashita, Y., Y. Tsukioka, Y. Nakano, K. Tomihisa, T. Oho, and T. Koga. 1998. Biological functions of UDP-glucose synthesis in *Streptococcus mutans*. Microbiology **144**:1235–1245.
64. Yang, Y. H., S. Dudoit, P. Luu, D. M. Lin, V. Peng, J. Ngai, and T. P. Speed. 15 February 2002, posting date. Normalization for cDNA microarray data: a robust composite method addressing single and multiple slide systematic variation. Nucleic Acids Res. **30**:e15. [Online.] <http://nar.oupjournals.org/cgi/content/full/30/4/e15>.
65. Yarwood, J. M., D. J. Bartels, E. M. Volper, and E. P. Greenberg. 2004. Quorum sensing in *Staphylococcus aureus* biofilms. J. Bacteriol. **186**:1838–1850.
66. Zhang, L., L. Gray, R. P. Novick, and G. Ji. 2002. Transmembrane topology of AgrB, the protein involved in the posttranslational modification of AgrD in *Staphylococcus aureus*. J. Biol. Chem. **277**:34736–34742.
67. Zhang, L., and G. Ji. 2004. Identification of a staphylococcal AgrB segment(s) responsible for group-specific processing of AgrD by gene swapping. J. Bacteriol. **186**:6706–6713.